This article has been accepted for publication in a future issue of this journal, but has not been fully edited. Content may change prior to final publication. Citation information: DOI 10.1109/JPHOT.2018.2856263, IEEE Photonics Journal

Generation of Orbital Angular Momentum Beam Using Fiber-to-Fiber Butt Coupling

Shuhui Li,[1] Zhe Xu,[1] Ruixuan Zhao,[1] Li Shen,[1] Cheng Du,[3] and Jian Wang[1,*]

[1]Wuhan National Laboratory for Optoelectronics, School of Optical and Electronic Information, Huazhong University of Science and Technology, Wuhan 430074, Hubei, China

[2]Fiberhome Telecommunication Technologies Co. Ltd, Wuhan, 430074, China.

[*] jwang@hust.edu.cn

Abstract: We experimentally demonstrate a simple scheme for broadband generation of orbital angular momentum (OAM) using a fiber-based structure. A standard single-mode fiber (SMF) is stuck to a two-mode fiber (TMF) with specific offsets and tilt angles to realize high-order fiber mode conversion. By adjusting the polarization controllers implemented on the SMF and TWF accompanied with a polarizer filter, one can selectively obtain LP_{11} mode or OAM modes with l=±1 at output end of the TMF. We show the high-purity (extinction ratio>20 dB) generation of OAM modes within a wide range from 1480 nm to 1640 nm.

Index Terms: Optical vortices，Fiber optics

1. Introduction

Orbital angular momentum (OAM) beams, also called optical vortex (OV) beams, are characterized by a helical phase front of $\exp(il\varphi)$ (l is the topological charge number and φ corresponds to the azimuth angle), have generated considerable interest in the recent past [1-4]. OAM beams have a number of applications in areas such as particle tapping, optical tweezers, sensing, imaging, and quantum informatics [2-8]. Very recently, OAM beams have also shown their potential use in communication systems to increasing transmission capacity and spectral efficiency [9-11].

For miscellaneous OAM-based applications, a key challenge has been the generation of OAM beams. Many approaches, such as cylindrical lens mode converters, q-plates, spiral phase plates, spatial light modulators (SLM), metamaterials-based phase plates, and silicon integrated devices have been proposed and demonstrated for generating OAM beams [1,3,12-14]. Besides, there is also an increasing interest in generation of OAM beams with optical fibers due to inherent advantages of fibers, like compactness, low cost, remote delivery and flexibility. Typically, there are three main approaches to generate OAM beams based on optical fibers: 1) grating structures, such as long-period fiber gratings formed by mechanical means, femtosecond laser direct writing, CO_2 or ultra-violet laser exposing, helical gratings, and acoustically induced gratings [15-19]; 2) coupler structures, like fused coupler fabricated from standard single mode fibers (SMFs) and OAM fibers, coupler structure of square core and ring refractive index profile [20, 21]; 3) facet structures or end-face exciting, for instance, fiber facets fabricated with metamaterials or micro spiral phase plates, coupling high-order linear polarized (LP) modes to stressed fibers, elliptical fibers or polarization maintaining fibers [22-26]. Despite the successful generation of OAM beams with optical fibers, one may also see several challenges: some methods are complex and difficult to form, some have a narrow bandwidth (e.g. reported bandwidth of fiber grating based OAM mode converter is less than 50 nm) [15,17], and the mode purity of some methods is not high. Therefore, it would be desirable to find a simple approach to realize broadband high-purity fiber-based OAM beam generation.

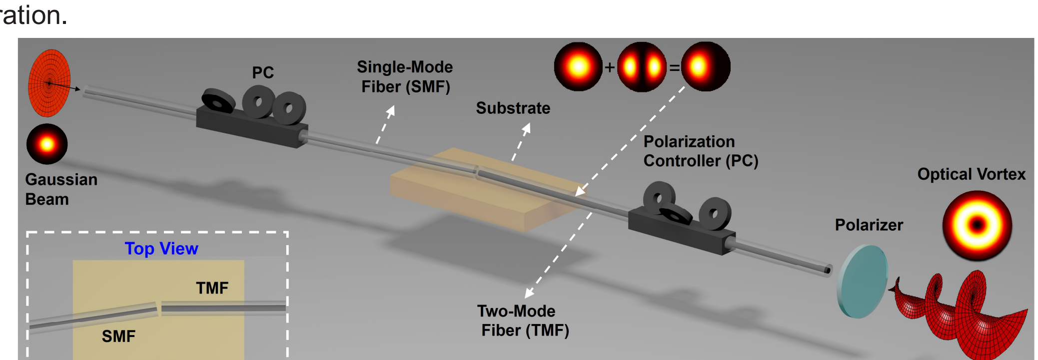

Fig. 1. Concept of controllable broadband fiber-based orbital angular momentum converter

In this paper, we propose and demonstrate a simple scheme to realize controllable broadband fiber-based OAM converter. The converter consists of a two-mode fiber (TMF) of which the input end is stuck to a standard SMF with optimized offsets and tilt angles, two polarization controllers (PCs) and one polarizer. By adjusting the two PCs, one can selectively convert an input fundamental mode to high-order LP_{11} mode or OAM modes with $l = \pm 1$. Through adjusting states of the two PCs and

This article has been accepted for publication in a future issue of this journal, but has not been fully edited. Content may change prior to final publication. Citation information: DOI 10.1109/JPHOT.2018.2856263, IEEE Photonics Journal

the polarizer, unconverted fiber fundamental mode component can be effectively filtered, ensuring a high mode purity. Extinction ratios between generated OAM modes and other modes are measured to evaluate the mode purity. The extinction ratio of larger than 20 dB of generated OAM modes is achieved within a wide wavelength range (1480 nm to 1640 nm).

2. Concept and principle

Converting the fundamental mode to high-order fiber modes and producing ±π/2 phase differences between even and odd high-order modes are two key issues for fiber-based OAM mode generation [16]. High-order fiber modes exciting can be achieved by asymmetric fiber-to-fiber butt coupling. When a SMF and a TMF are coaxial stuck or spliced together, most of the power will be coupled into the fundamental mode (LP_{01}), while the power of high-order modes (LP_{11}) is negligible. However, if there is a specific offset or tilt between the two fiber facets, as shown in Fig.1, partial power exiting from the SMF can be coupled to high-order modes of the TMF. According to the coupled mode theory [27], the input beam needs to match the fiber modes to ensure high coupling efficiency and low crosstalk. However, it is difficult to realize perfect excitation of LP_{11} mode simply through offset or tilt. The offset and tilt will excite LP_{01} and LP_{11} modes at the same time. When the offset is to a specific value (Fig.2(a)), the input intensity profile on the TMF facet is very similar to the interferogram of LP_{01} and LP_{11} mode with same power, as shown in Fig.2. Therefore, it is easier to excite this mode interference field. Significantly, after asymmetric coupling, the fundamental mode component can be filtered out with a polarizer accompanied with the PCs. The generated high-order modes at the output end of the TMF can be LP_{11} modes or OAM modes with $l = \pm 1$ relying on the phase difference between the two orthogonal mode components which can be controlled by appropriately adjusting the PCs [10]. Using PCs to adjust the directions of input mode and introduce birefringence between two orthogonal mode components has been widely used in OAM fiber-based transmission and generation applications [10, 15]. As there is no grating structure, it is believed that this configuration has a wide working bandwidth. Moreover, to make the configuration more robust, the asymmetric fiber-to-fiber butt coupling point can be spliced together or stuck on to a substrate, forming a compact device.

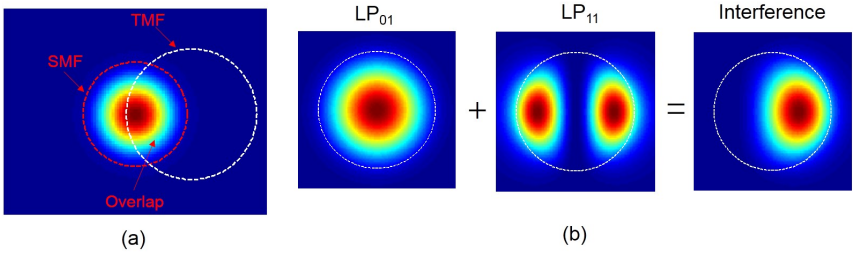

Fig. 2. (a) SMF and TMF with a specific offset. (b) Interferogram of LP_{01} and LP_{11} mode with same power

3. Experimental setup and results

The experimental setups for fabricating and testing the OAM beam converter using asymmetric fiber-to-fiber butt coupling are illustrated in Figs. 3 and 4. A regular horizontal fiber-to-waveguide butt coupling platform consisting of two 5-axis stages, a substrate holder, horizontal and vertical microscopic imaging system, is used to adjust the relative positions and tilt angles between the two fibers, as illustrated in Fig. 3(a). Fig. 3(b) is the top-view microscope image of the two fibers with a specific offset and tilt angle. One can find an optimized offset and tilt angle to achieve low-insertion-loss and high-purity OAM beams, by real-time monitoring the OAM mode quality through the setup displayed in Fig. 4. After the optimized position is found, the two fibers can be stuck on to a glass substrate with ultra-violet curing, as depicted in Fig. 3(c). The TMF used in this work is a custom-designed step index TMF with a core diameter of 15 μm and a 0.336% refractive index difference between the core and cladding. The fiber is optimized to stably support LP_{01} and LP_{11} mode transmission.

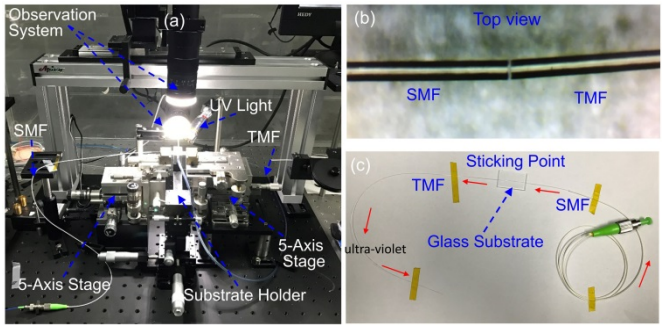

Fig. 3. (a) Platform for sticking a SMF to a TMF with specific offsets and tilt angles. (b) Microscope image of the butt coupling area (top view). (c) The fabricated fiber devices used for OAM beam conversion.

Figure 4 is the setup for testing the performance of fabricated fiber converters. The output beam from a tunable laser which having a bandwidth of 160 nm (1480 nm ~ 1640 nm) is divided into two paths by a 50:50 optical coupler. One path is used to generate OAM beams and the other path is used as a reference beam for interfering. After passing through the OAM beam converter, the output is collimated using a 20× objective lens, and fifty percent of the beam is imaged using a CCD camera to

This article has been accepted for publication in a future issue of this journal, but has not been fully edited. Content may change prior to final publication. Citation information: DOI 10.1109/JPHOT.2018.2856263, IEEE Photonics Journal

get the interference patterns, the other fifty percent of the beam is sent onto a spatial light modulator (SLM) for demodulation and power-spectrum measurement.

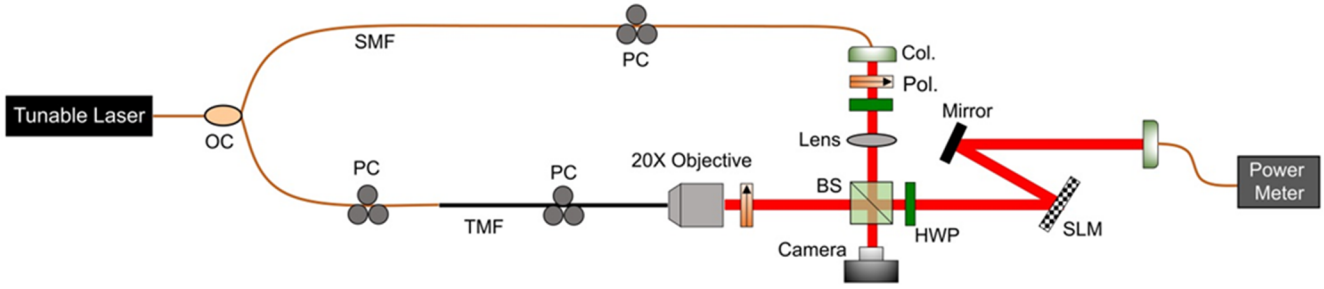

Fig. 4. Experiment setup for generation and detection of OAM beams using asymmetric fiber-to-fiber butt coupling. OC: optical coupler; PC: polarization controller; SMF: single-mode fiber; TMF: two-mode fiber; Col.: collimator; Pol.: polarizer; HWP: half-wave plate; BS: beam splitter; SLM: spatial light modulator.

Although asymmetric fiber-to-fiber butt coupling can excite high-order fiber modes, the conversion efficiency cannot reach 100%. There is still unnecessary fundamental mode component in the output beam, resulting in a low mode purity. Fortunately, the unnecessary fundamental mode component can be filtered out by a polarizer, as shown in Fig. 5. This is because that the polarization sates of high-order and fundamental fiber modes can be adjusted to be orthogonal through accommodating the two PCs.

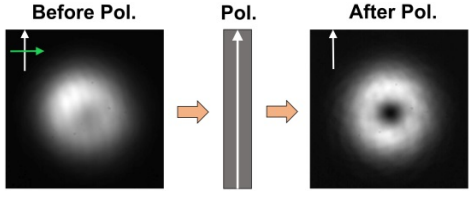

Fig. 5. Intensity profiles before and after the polarizer (pol.).

The intensity profile of a generated LP_{11} mode is displayed in Fig. 6 (a1). It can be clearly seen that the profile presents as two side lobe distribution, and the π phase jump can be recognised from the interferogram Fig. 6(a2). By appropriately adjusting the PCs, output beams can be OAM modes with $l = \pm 1$, as displayed in Fig. 5(b). Annular profiles can be clearly seen from Figs. 6(b1) and 6(b4). In order to confirm the helical phase structure, we interfere the generated OAM modes with a reference-spherical Gaussian beam. Shown in Figs. 6(b2) and 6(b5) are the interference patterns. The counter clockwise spiral interference pattern for $l = 1$ and the clockwise spiral interference pattern for $l = -1$ can be clearly observed from these figures, which indicate that OAM beams with $l = \pm 1$ are successfully achieved at the output terminal. When using reversed helical phase masks loaded onto the SLM to demodulate the OAM beams, there will emerge bright spots at the beam centres, as shown in Figs. 6(b3) and 6(b6).

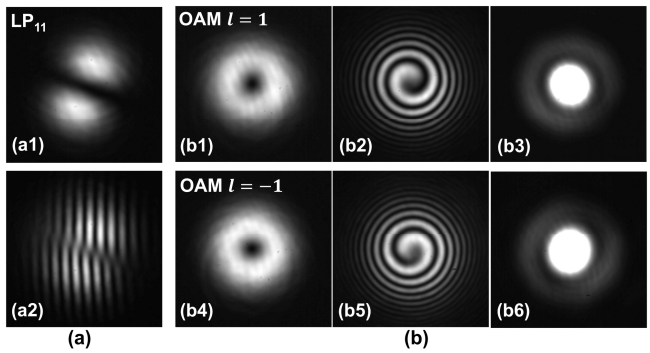

Fig. 6. (a) Intensity profile (a1) and interferogram (a2) of generated LP_{11} mode. (b) Intensity profiles, interferograms and demodulated profiles of generated OAM modes with $l = 1$ (b1-b3) and $l = -1$ (b4-b6).

In order to determine the optimal offsets and tilt angles for OAM beam generation, the power of generated OAM beams with different offsets and tilts is measured. Fig. 7(a) depicts the total received power (before the polarizer) and the power of OAM or LP_{11} beams (after the polarizer) with different offsets and a zero tilt angle. The input power is normalized to 0 dBm. It can be seen that the received total power decreases with the increase of offset (black curve). While the power of OAM beams increases first and reaches the maximum of -7.6 dBm near an offset of 3.5 μm, and then decreases (blue curve). Due to the incomplete conversion, the total received power includes both OAM beam component and unnecessary fundamental mode component. The power ratio of OAM beams relative to total received power is also display in Fig. 7(a) (red curve). One can find that the ratio also increases with the increase of offset firstly, and then almost becomes a constant. Moreover, to promote the conversion efficiency, tilts are also introduced to the asymmetric fiber-to-fiber butt coupling. Figs. 7(b) and 7(c) present the received power and power ratio of generated OAM beams with different tilt angles, respectively. These tilts can benefit both the received power of OAM beams and the power ratio. But the improvements are relatively small. The maximum conversion efficiency still arrives at about 3.5 μm which suggests that the offset takes a major role in the conversion. When the offset and the tilt angle are 3 μm and 2.7°, respectively, a maximum OAM-beam power of -4.7 dBm and a power ratio of

This article has been accepted for publication in a future issue of this journal, but has not been fully edited. Content may change prior to final publication. Citation information: DOI 10.1109/JPHOT.2018.2856263, IEEE Photonics Journal

-3.01 dB are obtained.

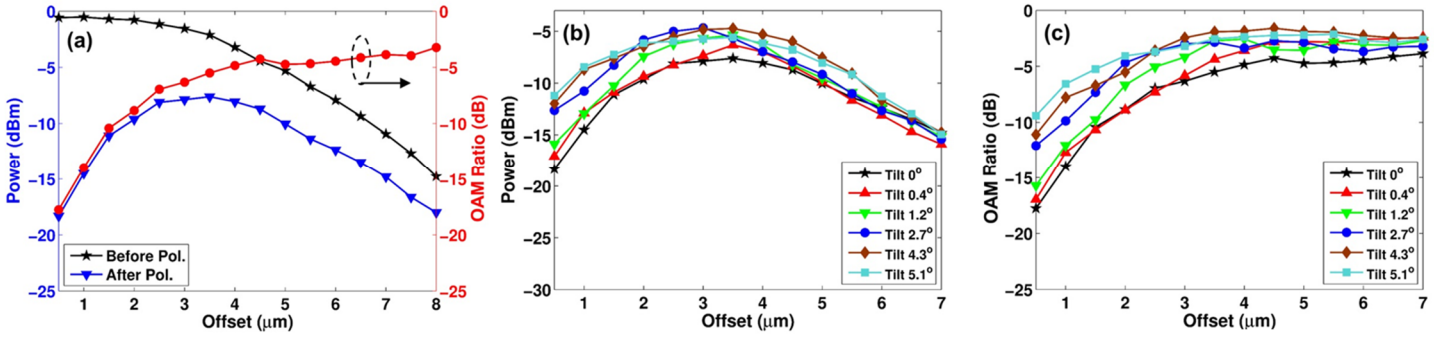

Fig. 7. (a) The total received power (before the polarizer) and power of OAM beams (after the polarizer) with different offsets and a zero tilt angle; power ratio of OAM beams relative to total received power (red curve). The received power (b) and power ratio (c) of generated OAM beams with different tilt angles as a function of offset.

Then the bandwidth performance of the proposed converter is tested. We measure the output power of one generated OAM mode ($l = 1$) at different input wavelength (1480 nm ~ 1640 nm), as illustrated in Fig. 8. The received power is fluctuant between -4.81 dBm and -6.26 dBm. The ratio between lowest and highest values is larger than -1.5 dB, indicating that this scheme has a wide working bandwidth. Moreover, the tested wavelength range is limited by the used tunable laser. The configuration can also have a favourable performance even out of this wavelength range.

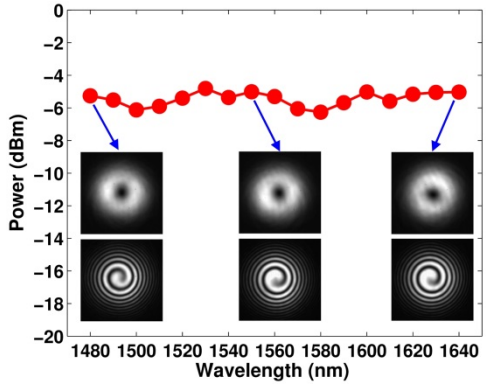

Fig. 8. Received power of generated OAM mode ($l = 1$) at different wavelength (1480 nm ~ 1640 nm).

Moreover, the mode purity of generated OAM modes are also evaluated. We measure the power spectrum of OAM modes with $l = \pm 1$ at three typical wavelengths (1480 nm, 1550 nm and 1640 nm). The power spectrum is measured by loading inverse phase mask with different charge number onto the SLM. Fig. 9 shows the measured results. One can see that the extinction ratios between generated OAM modes and other modes are larger than 21 dB. It suggests that most power is concentrated at the desired OAM modes, i.e. a high mode purity. This can also prove the effectiveness of using a polarizer accompanied with PCs to filter out the unnecessary fundamental mode component.

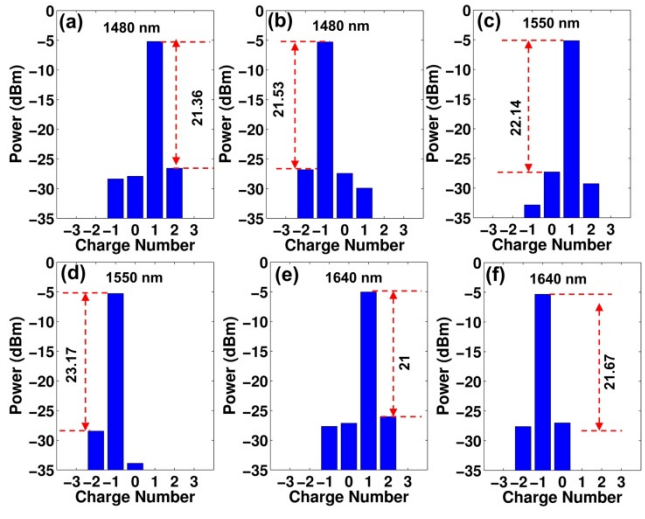

Fig. 9. Measured power spectrum of OAM modes with different charge number l at 1480 nm (a) (b), 1550 nm (c) (d) and 1640 nm (e) (f).

4. Conclusions

We have experimentally demonstrated a simple scheme for broadband generation of OAM beams using asymmetric fiber-to-fiber butt coupling. The fiber OAM converter is fabricated by sticking a SMF to a TMF with a specific offset and tilt

angle through a regular horizontal fiber-to-waveguide butt coupling platform and ultra-violet curing. The structure is compact and easy to process which can also be realized by asymmetric fused fiber splicing. Selective generation of LP_{11} mode or OAM modes with $l = \pm 1$ can be controlled by adjusting the PCs implemented on the SMF and TMF. To improve the mode purity, a polarizer cooperatively working with the PCs is employed to filter out unnecessary fundamental mode component. After polarization filtering, the extinction ratio of larger than 20 dB of generated OAM modes is achieved with in a wide wavelength range from 1480 nm to 1640 nm. In this simple approach, only partial power exiting from the SMF can be coupled into high-order modes of the TMF. Although the efficiency is not very high ($\approx$34%), the structure is fairly simple and the efficiency can be further improved. In order to reduce the loss, a vortex fiber laser can be built from this structure using a gain fiber. Moreover, pretreatments of fiber end may also help improve the power efficiency. It is feasible in theory to generate the OAM with $l = \pm 2$ or higher order if we change the optical fiber so that it can support higher order mode, but it makes controlling the purity more difficult. The asymmetric fiber-to-fiber butt coupling may excite multiple higher order modes simultaneously. Therefore，more complicated mode selection methods are needed to improve mode purity.The proposed simple, low-cost, controllable, and broadband fiber-based OAM beam converter may have a number of potential applications in fields, such as optical communications, optical manipulation, sensing and imaging.

Acknowledgements

This works was supported by National Natural Science Foundation of China (NSFC) (61705073, 61761130082, 11574001, 11274131, 61222502); National Basic Research Program of China (973 Program) (2014CB340004, 2014CB340003); Natural Science Foundation of Hubei Province of China (ZRMS2017000403, 2018CFA048); Shenzhen Strategic Emerging Industry Development Special Fund (JCYJ20170307172132582, JCYJ20160531194518142). Royal Society-Newton Advanced Fellowship; National Program for Support of Top-notch Young Professionals; Yangtze River Excellent Young Scholars Program; Program for HUST Academic Frontier Youth Team.

References

[1] L. Allen, M. W. Beijersbergen, R. J. C. Spreeuw, and J. P. Woerdman, "Orbital angular momentum of light and the transformation of Laguerre-Gaussian laser modes," Phys. Rev. A 45, 8185-8189 (1992).
[2] S. Franke-Arnold, L. Allen, and M. Padgett, "Advances in optical angular momentum," Laser Photonics Rev. 2, 299-313 (2008).
[3] A. M. Yao and M. J. Padgett, "Orbital angular momentum: origins, behavior and applications," Adv. Opt. Photonics 3, 161 (2011).
[4] M. J. Padgett, "Orbital angular momentum 25 years on [Invited]," Opt. Express 25, 11265 (2017).
[5] M. Padgett and R. Bowman, "Tweezers with a twist," Nat. Photonics 5, 343-348 (2011).
[6] M. P. J. Lavery, S. M. Barnett, F. C. Speirits, and M. J. Padgett, "Observation of the rotational Doppler shift of a white-light, orbital-angular-momentum-carrying beam backscattered from a rotating body," Optica 1, 1-4 (2014).
[7] S. W. Hell and J. Wichmann, "Breaking the diffraction resolution limit by stimulated emission: stimulated-emission-depletion fluorescence microscopy," Opt. Lett. 19, 780-782 (1994).
[8] X.-L. Wang, X.-D. Cai, Z.-E. Su, M.-C. Chen, D. Wu, L. Li, N.-L. Liu, C.-Y. Lu, and J.-W. Pan, "Quantum teleportation of multiple degrees of freedom of a single photon," Nature 518, 516-519 (2015).
[9] J. Wang, J.-Y. Yang, I. M. Fazal, N. Ahmed, Y. Yan, H. Huang, Y. Ren, Y. Yue, S. Dolinar, M. Tur, and A. E. Willner, "Terabit free-space data transmission employing orbital angular momentum multiplexing," Nat. Photonics 6, 488-496 (2012).
[10] N. Bozinovic, Y. Yue, Y. Ren, M. Tur, P. Kristensen, H. Huang, A. E. Willner, and S. Ramachandran, "Terabit-Scale Orbital Angular Momentum Mode Division Multiplexing in Fibers," Science 340, 1545-1548 (2013).
[11] J. Wang, "Advances in communications using optical vortices," Photonics Res. 4, B14 (2016).
[12] Z. Zhao, J. Wang, S. Li, and A. E. Willner, "Metamaterials-based broadband generation of orbital angular momentum carrying vector beams," Opt. Lett. 38, 932-934 (2013).
[13] L. Marrucci, C. Manzo, and D. Paparo, "Optical Spin-to-Orbital Angular Momentum Conversion in Inhomogeneous Anisotropic Media," Phys. Rev. Lett. 96, 163905 (2006).
[14] X. Cai, J. Wang, M. J. Strain, B. Johnson-Morris, J. Zhu, M. Sorel, J. L. O'Brien, M. G. Thompson, and S. Yu, "Integrated Compact Optical Vortex Beam Emitters," Science 338, 363-366 (2012).
[15] S. Ramachandran, P. Kristensen, and M. F. Yan, "Generation and propagation of radially polarized beams in optical fibers," Opt. Lett. 34, 2525-2527 (2009).
[16] S. Li, Q. Mo, X. Hu, C. Du, and J. Wang, "Controllable all-fiber orbital angular momentum mode converter," Opt. Lett. 40, 4376-4379 (2015).
[17] Y. Zhao, Y. Zhao, Y. Liu, C. Mou, N. Gordon, K. Zhou, L. Zhang, and T. Wang, "Femtosecond Laser Inscribed Axial Long-period Fiber Gratings in two-mode fiber for Efficient Optical Angular Momentum Generation," in Optical Fiber Communication Conference (2017), Paper W2A.14 (Optical Society of America, 2017), p. W2A.14.
[18] P. Z. Dashti, F. Alhassen, and H. P. Lee, "Observation of Orbital Angular Momentum Transfer between Acoustic and Optical Vortices in Optical Fiber," Phys. Rev. Lett. 96, (2006).
[19] G. K. L. Wong, M. S. Kang, H. W. Lee, F. Biancalana, C. Conti, T. Weiss, and P. S. J. Russell, "Excitation of Orbital Angular Momentum Resonances in Helically Twisted Photonic Crystal Fiber," Science 337, 446-449 (2012).
[20] S. Pidishety, B. Srinivasan, and G. Brambilla, "All-Fiber Fused Coupler for Stable Generation of Radially and Azimuthally Polarized Beams," IEEE Photonics Technol. Lett. 29, 31-34 (2017).
[21] Y. Yan, L. Zhang, J. Wang, J.-Y. Yang, I. M. Fazal, N. Ahmed, A. E. Willner, and S. J. Dolinar, "Fiber structure to convert a Gaussian beam to higher-order optical orbital angular momentum modes," Opt. Lett. 37, 3294-3296 (2012).
[22] X. Wang, J. Zeng, J. Sun, V. F. Nezhad, A. N. Cartwright, and N. M. Litchinitser, "Metasurface-on-fiber enabled orbital angular momentum modes in conventional optical fibers," in CLEO: Applications and Technology (Optical Society of America, 2014), p. JTu4A-34.
[23] I. Weiss and D. M. Marom, "Direct 3D nanoprinting on fiber tip of collimating lens and OAM mode converter in one compound element," in Optical Fiber Communication Conference (Optical Society of America, 2016), p. Th3E-2.
[24] R. D. Niederriter, M. E. Siemens, and J. T. Gopinath, "Continuously tunable orbital angular momentum generation using a polarization-maintaining fiber," Opt. Lett. 41, 3213 (2016).
[25] D. McGloin, N. B. Simpson, and M. J. Padgett, "Transfer of orbital angular momentum from a stressed fiber-optic waveguide to a light beam," Appl. Opt. 37, 469-472 (1998).
[26] A. N. Alexeyev, C. N. Alexeyev, E. G. Galamaga, A. V. Volyar, and M. A. Yavorsky, "Generic optical vortex in a strongly elliptic optical fibre," in (SPIE, 2005), Vol. 6023, p. 60230S-60230S-8.
[27] A. Snyder and J. Love, Optical waveguide theory (Kluwer Academic Publishers, 2000).